

Constructal Theory: Tree-Shaped Flows and Energy Systems for Aircraft

Adrian Bejan*

Duke University, Durham, North Carolina 27708-0300

Attention is drawn to constructal theory and design, which relies on global maximization of performance in the pursuit of flow system architecture. Exergy analysis establishes the theoretical performance limit. Thermodynamic optimization (or entropy generation minimization) brings the design as closely as permissible to the theoretical limit. The design is destined to remain imperfect because of constraints (finite sizes, times, and costs). Improvements are registered by spreading the imperfection, for example, flow resistances, through the system. Resistances compete against each other and must be optimized together. Optimal spreading means geometric form. System architecture is generated by the constructal principle: constrained global optimization and constraints in a morphing flow medium. In flows that connect a volume (or area) with one point, the resulting structure is a tree of low-resistance links, and high-resistance interstices. These structures are robust, diverse, and everywhere. A key example is the extraction of maximum exergy from a hot-gas stream that is cooled and discharged into the ambient. The optimal configuration consists of a heat transfer surface with a temperature that decays exponentially in the flow direction. Additional examples show that the complete structure of a heat exchanger for an environmental control system can be derived based on this method.

Introduction

THE methods of exergy analysis (EA), entropy generation minimization (EGM), and thermoeconomics (TE) are the most established changes that have taken place in contemporary engineering thermodynamics teaching and practice.^{1–12} The emphasis today is on identifying the mechanisms and system components that are responsible for thermodynamic losses (EA), the size of each loss (EA), the minimization of losses subject to global constraints (EGM), the development of system architecture based on global thermodynamic optimization (EGM), and the minimization of the costs due to building and operating the energy system (TE).

Exergy analysis is pure thermodynamics. It relies on the laws of thermodynamics to establish the theoretical limit of ideal (reversible) operation and the extent to which the operation of the given (actual, specified) system departs from the ideal. The departure is measured by the calculated quantity called destroyed exergy, or irreversibility. This quantity is proportional to the generated entropy. Exergy is the thermodynamic property that describes the “useful energy” content, or the “work producing potential” of substances and streams. In real systems, exergy is always destroyed, partially or totally, when components and streams interact.

Thermodynamic optimization (EGM) is the minimization of exergy destruction or entropy generation.^{2,10} This design activity requires the use of more than thermodynamics: Fluid mechanics, heat and mass transfer, materials, constraints, and geometry are also needed to establish the relationships between the physical configuration and the destruction of exergy. Reductions in exergy destruction are pursued through changes in configuration. The resistances faced by various streams are minimized and balanced together. The thermodynamic imperfection is distributed. In the end, the configuration emerges as the result of the global optimization of thermodynamic

performance subject to global constraints. This is called *constructal theory and design*.¹

Thermodynamic optimization may be used by itself, without cost minimization, to identify trends and tradeoffs, the existence of optimization opportunities. The configurations identified based on thermodynamic optimization can be made more realistic through subsequent refinements based on more representative models and based on global cost minimization.¹¹ The integrative constructal design philosophy that emerges is one where the entire system can be conceived of as a construct designed to meet a global objective optimally, not as an ensemble of already existing parts. In this paper, two classes of applications where the flow-system architecture results from global thermodynamic optimization are reviewed.

Tree-Shaped Paths for Volume-Point Flows

In this section, a newly emerging body of work that describes the flow between a finite size volume (or area) and a single point (source, or sink) is reviewed. This work goes well beyond the description (calculation) of the flow resistance associated with the flow path: The new and primary focus is on optimizing geometrically the flow path, so that the global volume-point resistance is minimum. The flow path that results from geometric optimization is shaped as a tree.

What flows along the tree links is not nearly as important as how the geometric form “tree” is generated by the geometric optimization principle. Dissipative structures are deducible from principle. This is important: The generation of geometric form is a phenomenon that is accounted for by principle. The generation of trees for heat flow, fluid flow, combined heat and fluid flow, electricity (e.g., lightning and circuitry), people and goods (e.g., streets and highways), and communications is reviewed in Ref. 1. The thought that the geometric optimization principle accounts not only for engineered flows, but also for the billions of tree-shaped flows of nature, was named constructal theory.¹

In the constructal optimization of the volume-to-point path for heat flow, it was shown that a volume subsystem of any size can have its external shape and internal details optimized such that its own volume-to-point resistance is minimal.^{1,13,14} This principle is repeated in the optimization of volumes of increasingly larger scales, where each new volume is an assembly of previously optimized smaller volumes. The construction spreads as the assemblies cover larger spaces.

Presented as Paper 2000-4855 at the AIAA/USAF/NASA/ISSMO 8th Symposium on Multidisciplinary Analysis, Long Beach, CA, 8 September 2000; received 23 January 2001; revision received 17 July 2002; accepted for publication 18 July 2002. Copyright © 2002 by Adrian Bejan. Published by the American Institute of Aeronautics and Astronautics, Inc., with permission. Copies of this paper may be made for personal or internal use, on condition that the copier pay the \$10.00 per-copy fee to the Copyright Clearance Center, Inc., 222 Rosewood Drive, Danvers, MA 01923; include the code 0021-8669/03 \$10.00 in correspondence with the CCC.

*J. A. Jones Professor of Mechanical Engineering, Department of Mechanical Engineering and Materials Science.

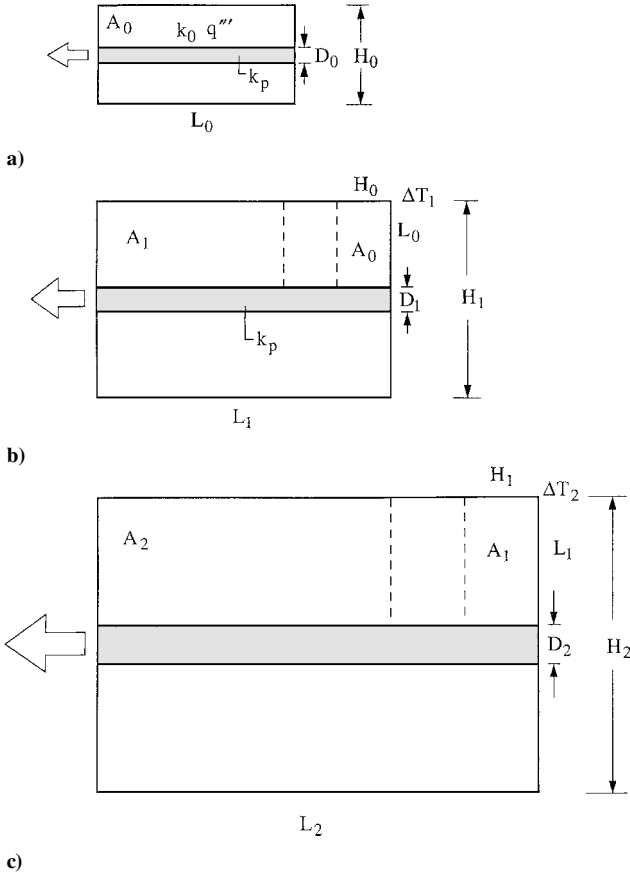


Fig. 1 Constructal growth: the minimization of thermal resistance via spatial growth.¹⁵

As an example, consider the flow of heat from a volume to one point. The heat-flow geometry is two dimensional. The low-conductivity material k_0 generates heat volumetrically at the rate q''' , which is assumed uniform. A small (fixed) amount of high-conductivity material k_p is to be distributed through the k_0 material. The construction begins with the smallest volume scale (the elemental system), which is represented by the rectangular area $A_0 = H_0 L_0$. The start of this sequence of volume sizes is shown in Fig. 1a (see Ref. 15). The A_0 size is known and fixed, for example, in the conduction cooling of an electronic material, A_0 is the smallest size that is allowed by manufacturing and electrical design constraints. The A_0 system is “elemental” because it has only one insert of high-conductivity material. This blade has the thickness D_0 , and it is positioned on the long axis of the $H_0 \times L_0$ rectangle. The heat current $q''' A_0$ is guided out of A_0 through the left end of the D_0 channel, which is the heat sink. The hot spots occur in the right-hand corners.

The global volume-to-point resistance is the ratio $\Delta T_0/(q''' A_0)$, where ΔT_0 is the temperature difference between the hot spot and the heat sink. This measure is “global” because the heat current $q''' A_0$ is integrated over the system A_0 , and the maximum temperature difference ΔT_0 is the excess temperature of the hot spot, or hot spots, of the entire system. The location of the hot spots is not an issue, as long as they reside inside the system. The global resistance refers to the entire system and its ability to accommodate the volume-to-point flow without violating the requirement that the hot spots do not exceed a certain temperature ceiling.

The composite material that fills A_0 is characterized by two dimensionless numbers, the conductivity ratio $\tilde{k} = k_p/k_0$, and the volume fraction of high-conductivity material, $\phi_0 = D_0/H_0$. It was shown that when $\tilde{k} \gg 1$ and $\phi_0 \ll 1$ the volume-to-point resistance is given by the two-term expression^{1,13}

$$\Delta T_0 k_0 / q''' A_0 = \frac{1}{8} \cdot (H_0/L_0) + (1/2\tilde{k}\phi_0) \cdot (L_0/H_0) \quad (1)$$

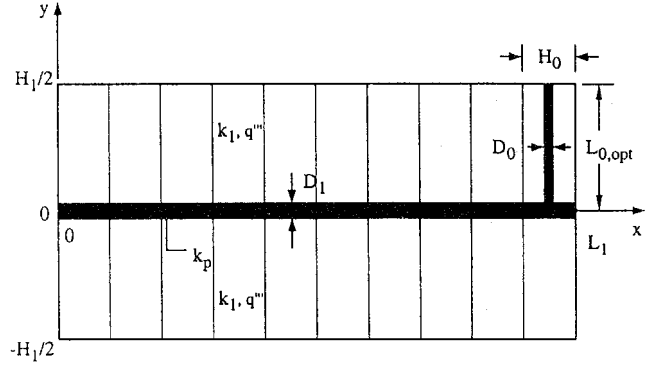


Fig. 2 First construct: a large number of elemental volumes connected to a central high-conductivity path.^{1,13}

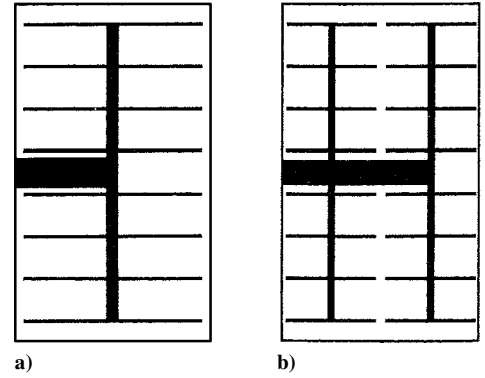


Fig. 3 Second-construct geometry optimized numerically ($\phi_2 = 0.1$, $\tilde{k} = 300$, and $n_1 = 8$): a) $n_2 = 2$ and b) $n_2 = 4$ (Ref. 16).

This resistance is minimal when the shape of A_0 is

$$(H_0/L_0)_{\text{opt}} = 2(\tilde{k}\phi_0)^{-\frac{1}{2}} \quad (2)$$

The construction continues with the first assembly (A_1 , Fig. 1b), which contains n_1 elemental systems, $A_1 = n_1 A_0$. The resulting structure is shown in greater detail in Fig. 2. The heat currents produced by the elemental systems are collected by a new high-conductivity insert of thickness D_1 , the left end of which is the heat sink. The hot spot is in the two right-hand corners. The volume-to-point resistance is $\Delta T_1/(q''' A_1)$, where ΔT_1 is the excess temperature at the hot spot. It was shown that the resistance can be minimized with respect to the shape parameter H_1/L_1 and the internal ratio D_1/D_0 .

The same geometric optimization principle applies at larger scales. The next scale is the second construct A_2 (Fig. 1c), which contains a number n_2 of first constructs, $A_2 = n_2 A_1$. The optimal external aspect ratio of the second construct is $H_2/L_2 = 2$, as in the two examples given in Fig. 3. Note the optimized internal ratios of high-conductivity blade thicknesses, D_1/D_0 and D_2/D_1 , where D_2 is the thickness of the central (thickest and newest) blade.

The geometrically optimal construction started in Figs. 1–3 can be continued to higher orders of assembly, until the structured composite (k_0, k_p) covers the given space. One interesting feature in this limit is that the construction settles into a recurring pattern of pairing (or bifurcation, from the reverse time direction), in which the integer 2 is a result of geometric optimization. For example, Fig. 3a shows this pairing and size doubling pattern. The geometric parameters, volume fractions occupied by high-conductivity material, and the global resistances of constructs up to the sixth level, are reported analytically in tabular form in Refs. 1, 12 and 13.

The heat trees of Figs. 1–3 do not look entirely “natural.” This is due to the simplifying assumptions on which their derivation was based: The high-conductivity inserts were always drawn with constant thickness and perpendicular to their tributaries. These features served their purpose. They kept the number of geometric degrees

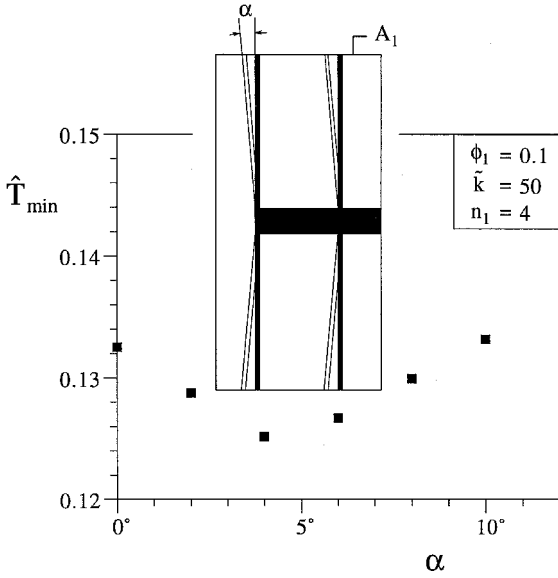


Fig. 4 Optimization of the angle of confluence between tributaries and their common stem in a first construct ($\phi_1 = 0.1$, $\tilde{k} = 50$, and $n_1 = 4$) (Ref. 17).

of freedom to a minimum, and, in this way, they made possible the closed-form presentation of the geometric optimization.

Constructal trees look more and more natural if their freedom to provide easier access to their internal currents is expanded. In the elemental system of Fig. 1a, it was assumed that the k_p channel stretches all of the way across the volume. When this assumption is not made, we find numerically that there is an optimal spacing between the tip of the k_p channel and the adiabatic boundary of the elemental volume.¹⁶

Another example is the angle formed between each tributary channel, and its central stem is allowed to vary. Numerical calculations of the two-dimensional heterogeneous conduction field show that there exists an optimal angle for minimal volume-to-point resistance at the construct level.¹⁷ This effect is illustrated for a first construct in Fig. 4, where, for simplicity, it was assumed that all of the tributaries are tilted at the same (variable) angle. The volume-to-point resistance of the construct, $\hat{T} = (T_{\max} - T_{\min})(k_0/q'' A_1)$ decreases only marginally (by 5.8%) as the angle α changes from the perpendicular position ($\alpha = 0$ deg) to the optimal position ($\alpha \cong 4$ deg).

These relatively unimportant improvements tell a very important story: The tree design is robust with respect to various modifications in its internal structure. This means that the global performance of the system is relatively insensitive to changes in some of the internal geometric details. Trees that are not identical have nearly identical performance and nearly identical macroscopic features such as the external shape.¹

Robustness continues to impress as we increase the number of degrees of freedom of the geometric design. In Fig. 5 we see the results of a fully numerical optimization of the second construct with perpendicular and constant-thickness inserts D_0 , D_1 , and D_2 , where all of the other geometric parameters were allowed to vary, the aspect ratios of all of the rectangles, large and small, the number of elemental volumes in each first construct n_1 , and the number of first constructs in each second construct n_2 . The three designs shown in Fig. 5 have been optimized with respect to all of the free parameters except n_2 , and they have been drawn to scale [$n_{1,\text{opt}} = 8$, $(D_1/D_0)_{\text{opt}} = 5$, and $(D_2/D_0)_{\text{opt}} = 10$]. Figure 5 shows visually the effect of fine tuning the number of first constructs incorporated in the second construct n_2 .

The same effect is documented numerically in Table 1. The size of the second construct ($A_2 = H_2 L_2$) is fixed. The cold spot (T_{\min}) is at the root of the tree, and the two hot spots are in the farthest (left-side) corners. The aspect ratio H_2/L_2 refers to the vertical/horizontal external dimensions of the largest rectangle. The best second construct is the one with $n_2 = 4$; however, the neighboring designs ($n_2 = 2, 6$)

Table 1 Effect of increasing the number of first constructs n_2 in the optimized second construct when $\phi_2 = 0.1$ and $\tilde{k} = 300$ (Ref. 17)

n_2	$(T_{\max} - T_{\min})_{\min} k_0 / (q'' A_2)$	$(H_2/L_2)_{\text{opt}}^{1/2}$
2	0.0379	1.412
4	0.0354	1.375
6	0.0374	1.360

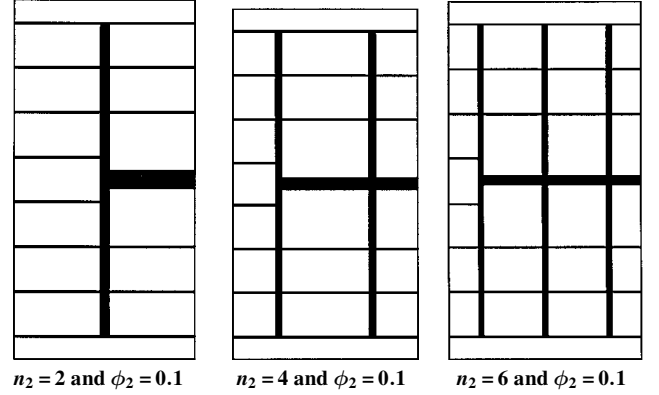


Fig. 5 Second construct optimized numerically¹⁷ for minimum resistance in volume-point steady flow and the effect of changing the number of first constructs n_2 . (See also Table 1.)

perform nearly as well. The global resistances of all of these designs agree within 7%, even though their internal structures are markedly different. Their optimized external shapes are also nearly the same.

In summary, the global optimization principle leads us to very robust (invariant) features such as the global performance level and the external shape of the construct. Changes in the internal tree structure, such as overgrowth and surgery (adding or cutting branches) has almost no effect on the globally optimized features. These characteristics are explored further in Ref. 1.

Maximum Exergy from a Stream of Hot Gas

In classical engineering thermodynamics, it is assumed routinely that the energy input that drives a power plant is already available as heat transfer from a high-temperature reservoir. On an aircraft, the exergy supply is provided by a stream of fuel that is being burned. If the destruction of exergy during combustion is unavoidable, then the most that we have at our disposal is a stream of hot products of combustion. The stream becomes progressively colder as its exergy is being extracted by the power conversion system.

Thermodynamics alone provides an unambiguous answer to the question of the maximum power that is theoretically available from a stream solely in the presence of the atmospheric temperature reservoir T_0 : That answer is the "flow exergy" of the stream.^{3,5} It is helpful to review this result while looking at the upper part of Fig. 6 (see Ref. 18) and assuming that the stream is single phase, for example, an ideal gas. If the hot stream (\dot{m} , T_H) makes contact with a reversible device while reaching thermal equilibrium with the ambient before it is discharged, and if the pressure drop along the stream is assumed negligible, the power output is

$$\dot{W}_{\text{rev}} = \dot{m} c_p T_0 [T_H/T_0 - 1 - \ln(T_H/T_0)] \quad (3)$$

The actual power output will always be lower than \dot{W}_{rev} because of the irreversibility of the heat transfer between the hot stream and the rest of the power plant. A first step in the direction of accounting for the heat transfer irreversibility is the model of Fig. 6, where the heat transfer surface has the finite size $A = pL$, where p is the heat transfer area per unit of flowpath length. The power producing compartment is a succession of many reversible compartments of the kind shown in the center of the Fig. 6. The infinitesimal power output is where the temperature is plotted on the vertical in Fig. 6, and $d\dot{Q}_H = \dot{m} c_p dT$:

$$d\dot{W} = [1 - T_0/T_s(x)] d\dot{Q}_H \quad (4)$$

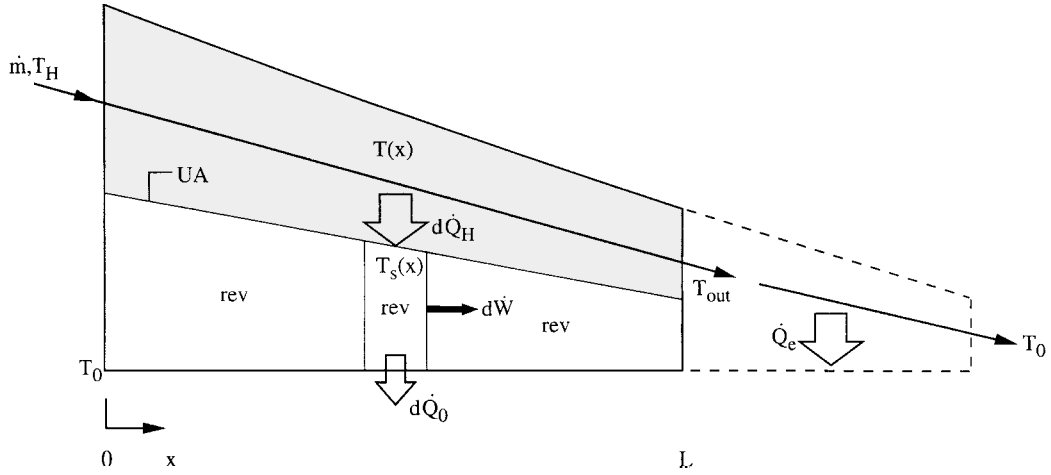


Fig. 6 Power plant model with unmixed hot stream in contact with nonisothermal heat transfer surface.¹⁸

The heat transfer through the surface A is assumed proportional to the local temperature difference,

$$d\dot{Q}_H = [T(x) - T_s(x)]U p dx \quad (5)$$

where U is the overall heat transfer coefficient, which is assumed constant. Combining these equations and integrating from $x = 0$ to $L (= A/p)$, we arrive at the total power output and the finite area constraint:

$$\dot{W} = \int_{T_{out}}^{T_H} \left(1 - \frac{T_0}{T_s}\right) \dot{m} c_p dT \quad (6)$$

$$\int_{T_{out}}^{T_H} \frac{dT}{T - T_s} = \frac{UA}{\dot{m} c_p} = N_{tu} \quad (7)$$

An alternate route to calculating the power output \dot{W} is to apply the Gouy–Stodola theorem to the larger system (extended with dashed line) in Fig. 6: $\dot{W} = \dot{W}_{rev} - T_0 \dot{S}_{gen}$. The reversible-limit power output \dot{W}_{rev} corresponds to the reversible cooling of the stream from T_H all of the way down to T_0 . The entropy generation rate \dot{S}_{gen} is the total amount associated with the larger system and is due to two sources, the temperature difference $T - T_s$ and the finite temperature difference required by the external cooling rate $\dot{Q}_e = \dot{m} c_p (T_{out} - T_0)$.

To maximize \dot{W} is equivalent to minimizing \dot{S}_{gen} because \dot{W}_{rev} is fixed. There are two degrees of freedom, the shape of the function $T_s(x)$ and the place of this function on the temperature scale, that is, closer to T_H or T_0 . The second degree of freedom is alternately represented by the value of the exhaust temperature T_{out} .

The optimization of the function $T_s(x)$ is accomplished based on variational calculus subject to the constraint (7) (Ref. 18). At any x , the temperature difference $(T - T_s)$ is proportional to the local absolute temperature. This optimal distribution of temperatures is illustrated in Fig. 7.

The second step of the minimization of exergy destruction consists of optimizing numerically the value of T_{out} . The result is the twice-maximized power output $\dot{W}_{max,max}$ reported in dimensionless form in Fig. 8,

$$\tilde{W}_{mm} = \dot{W}_{max,max} / (\dot{m} c_p T_0) \quad (8)$$

The deduced proportionality between $(T - T_s)$ and T (or T_s) means that this optimal configuration can be implemented in practice by using a single-phase stream $(\dot{m} c_p)_s$ in place of the $T_s(x)$ surface: This stream runs in counterflow relative to the hot stream \dot{m} . The counterflow is characterized by a certain, optimal imbalance (the ratio between the capacity flow rates of the two streams), which is the result of thermodynamic optimization (Fig. 9).

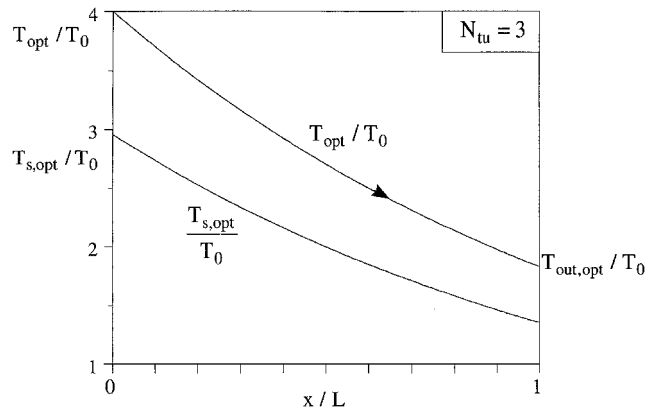


Fig. 7 Optimal distribution of temperature along the stream and the heat transfer surface of Fig. 6 (Ref. 18).

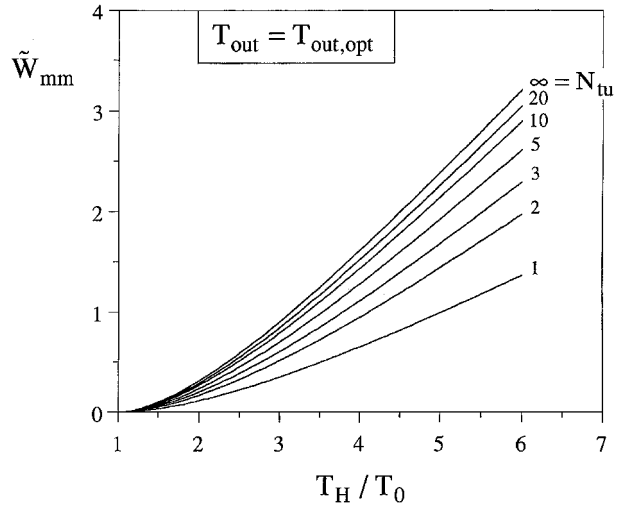


Fig. 8 Twice maximized power output corresponding to the model of Fig. 6 (Ref. 18).

In conclusion, extraction of power from a hot stream can be maximized by properly matching the stream with a receiving stream of cold fluid, across a finite size heat transfer area. This optimization opportunity deserves to be pursued in considerably more complex energy system configurations. For example, when the cold stream for example, water, evaporates as it captures a part of the hot-stream exergy, its side of the heat exchanger is divided optimally into three sections: liquid preheating, boiling, and vapor superheating for example, Fig. 10. These sections adjust themselves to their proper relative sizes as the system approaches the global thermodynamic

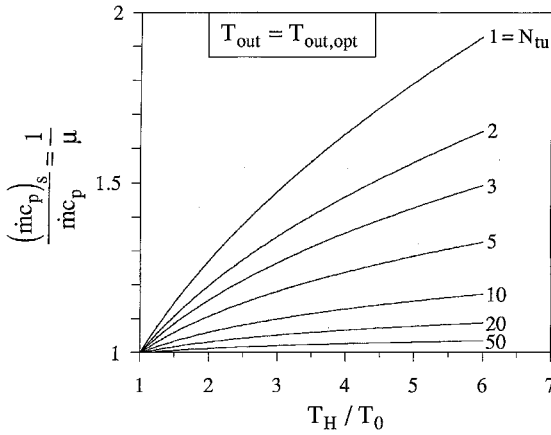


Fig. 9 Optimal imbalance of the counterflow heat exchanger used in conjunction with the model of Fig. 6 (Ref. 18).

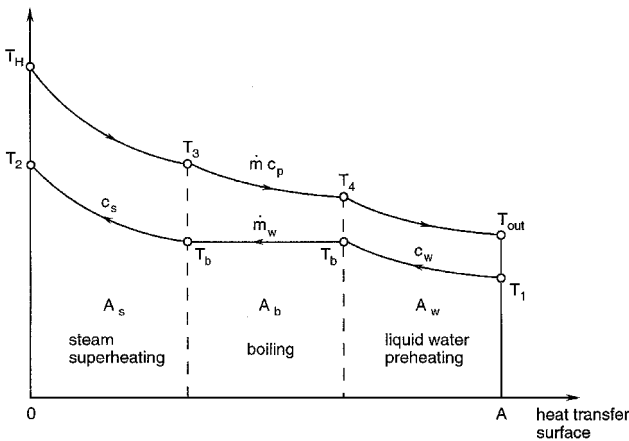


Fig. 10 Temperature distributions along a counterflow heat exchanger where the cold stream experiences phase change.¹⁹

optimum. This arrangement was analyzed and optimized in detail by Vargas et al.¹⁹

The model of Fig. 6 was only an example of how to start a conceptual design based on exergy analysis and subsequent optimization. The start was the extraction of exergy from a nonisothermal stream of hot gases subject to size constraints. To make this principle clear, we relied on the simplest possible model. Even at this early stage, we saw that an optimal configuration emerges and that its features are robust. This body of work points in several directions for future research. Beyond the simple models and analyses illustrated in this paper, we must consider the actual structure (dimensions, passages, fins) of the heat transfer surface that separates the exergy source stream from the rest of the installation. Another direction is the optimization of the structure that uses the extracted exergy, the arrangement of components that in Fig. 6 reside under the surface $T_s(x)$. A challenge is the number of degrees of freedom, which increases as the complexity of the contemplated system increases. Relevant to this is whether the thermodynamic optima of simpler systems are robust enough to reappear at least approximately in larger assemblies. In such cases, the results obtained for simpler systems can be used as shortcuts in the optimization of larger and more complex constructs.

Constructal Law of Maximal Access: Flow Architecture from Global Optimization

In this paper we focused on energy systems for aircraft. Indeed, by minimizing the power required for sustaining flight, it is possible to predict the observed cruising speeds of all of the bodies that fly, natural and engineered (Fig. 11) (Ref. 1). The theoretical cruising speed V is proportional to the body mass M raised to the power $\frac{1}{6}$. The same principles apply to designs in which all of the functions are driven by the exergy drawn from the limited fuel installed onboard: ships, automobiles, military vehicles, environmental-control suits, portable power tools, weapon systems, etc.

The performance record of the natural and engineered designs (Figs. 5 and 11) suggests that the principle invoked in this paper (constructal law) is important not only in engineering, but also in physics and biology, in general. In this theoretical framework, the airplane emerges as a physical extension of man, in the same way that

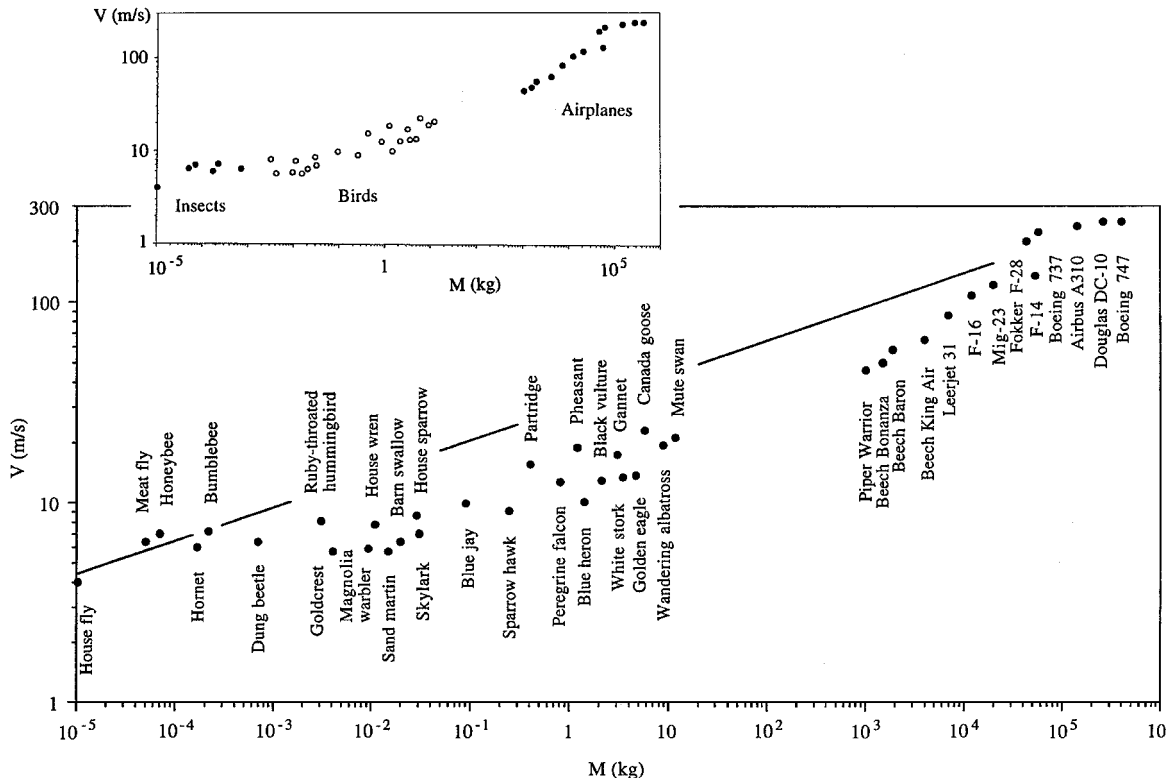


Fig. 11 Cruising speeds of insects, birds, and airplanes and the speed for minimum rate of exergy destruction.¹

the body of the flying animal (e.g., bat, bird, or insect) developed its own well-adapted extensions. All such extensions are discrete marks on a continuous time axis that points toward the better and the more complex.^{1,12–14}

Optimal distribution of imperfection is the constructal principle that generates form. (Further discussions of constructal theory are provided in Refs. 20–22.) The system is destined to remain imperfect. The system works best when its imperfection (internal flow resistances, irreversibilities) is spread around, so that more and more of the internal points are stressed as much as the hardest working points. The more we think of engineered systems in this way, the more these systems look and function like animals.

Conclusions

Constructal theory is a general and purely mental viewing that accounts for organization, complexity, and diversity in nature, engineering, and management. The constructal law was first stated in 1996, in the context of optimizing the access to flow between a point and an area, with application to traffic¹⁴ and the cooling of electronics¹³: “For a finite-size open system to persist in time (to survive) it must evolve in such a way that it provides easier and easier access to the currents that flow through it.” What flows, heat, fluid, people, and goods, is not nearly as important as how the flow derives its macroscopically visible structure from global objective, all in a malleable, changing, and morphing medium.

Acknowledgment

This material is based upon work supported by the Air Force Office of Scientific Research under Contract F49620-98-C-0007. Any opinions, findings and conclusions, or recommendations are those of the authors and do not necessarily reflect the views of the Air Force Office of Scientific Research. The author acknowledges with gratitude the guidance provided in this research project by David L. Siems of the The Boeing Company.

References

- ¹Bejan, A., *Shape and Structure, from Engineering to Nature*, Cambridge Univ. Press, Cambridge, England, U.K., 2000.
- ²Bejan, A., *Entropy Generation Through Heat and Fluid Flow*, Wiley, New York, 1982.
- ³Moran, M. J., *Availability Analysis: A Guide to Efficient Energy Use*, Prentice-Hall, Englewood Cliffs, NJ, 1982.
- ⁴Feidt, M., *Thermodynamique et Optimisation Énergetique des Systèmes*

et Procédés, Technique et Documentation, Lavoisier, Paris, 1987.

- ⁵Bejan, A., *Advanced Engineering Thermodynamics*, Wiley, New York, 1988.
- ⁶Stecco, S. S., and Moran, M. J., *Energy for the Transition Age*, Nova Science, New York, 1992.
- ⁷Richter, H. J. (ed.), *Thermodynamics and the Design, Analysis, and Improvement of Energy Systems 1993*, HTD-Vol. 266, American Society of Mechanical Engineers, New York, 1993.
- ⁸Krane, R. J. (ed.), *Thermodynamics and the Design, Analysis, and Improvement of Energy Systems 1994*, AES-Vol. 33, American Society of Mechanical Engineers, New York, 1994.
- ⁹Moran, M. J., and Sciubba, E., “Exergetic Analysis: Principles and Practice,” *Journal of Engineering for Gas Turbines and Power*, Vol. 116, No. 2, 1994, pp. 285–290.
- ¹⁰Bejan, A., *Entropy Generation Minimization*, CRC Press, Boca Raton, FL, 1996.
- ¹¹Bejan, A., Tsatsaronis, G., and Moran, M., *Thermal Design and Optimization*, Wiley, New York, 1996.
- ¹²Bejan, A., *Advanced Engineering Thermodynamics*, 2nd ed., Wiley, New York, 1997, Chap. 13.
- ¹³Bejan, A., “Constructal-Theory Network of Conducting Paths for Cooling a Heat Generating Volume,” *International Journal of Heat and Mass Transfer*, Vol. 40, No. 4, 1997, pp. 799–816.
- ¹⁴Bejan, A., “Street Network Theory of Organization in Nature,” *Journal of Advanced Transportation*, Vol. 30, No. 2, 1996, pp. 85–107.
- ¹⁵Bejan, A., and Dan, N., “Two Constructal Routes to Minimal Heat Flow Resistance via Greater Internal Complexity,” *Journal of Heat Transfer*, Vol. 121, No. 1, 1999, pp. 6–14.
- ¹⁶Almogbel, M., and Bejan, A., “Conduction Trees with Spacings at the Tips,” *International Journal of Heat and Mass Transfer*, Vol. 42, No. 20, 1999, pp. 3739–3756.
- ¹⁷Ledezma, G. A., Bejan, A., and Errera, M. R., “Constructal Tree Networks for Heat Transfer,” *Journal of Applied Physics*, Vol. 82, No. 1, 1997, pp. 89–100.
- ¹⁸Bejan, A., and Errera, M. R., “Maximum Power from a Hot Stream,” *International Journal of Heat and Mass Transfer*, Vol. 41, No. 13, 1998, pp. 2025–2035.
- ¹⁹Vargas, J. V. C., Ordonez, J. C., and Bejan, A., “Thermodynamic Optimization of Power Extraction from a Hot Stream in the Presence of Phase Change,” *International Journal of Heat and Mass Transfer*, Vol. 43, No. 2, 2000, pp. 191–201.
- ²⁰Rossiter, A., “Shape and Structure, from Engineering to Nature,” *Chemical Engineering Progress*, Feb. 2002, p. 81.
- ²¹Riznic, J., “Search for Better Performance Has Wide Appeal,” *Engineering Dimensions*, July/Aug. 2001, pp. 40, 41.
- ²²Cervantes de Gortari, J., “Shape and Structure, from Engineering to Nature,” *International Journal of Heat and Mass Transfer*, Vol. 45, No. 7, 2002, p. 1583.